Journal of the European Ceramic Society **19** (1999) 1979–1985

PII: S0955-2219(99)00015-1
0955-2219/99/$ - see front matter

Photoacoustic Thermal Characterization of Electrical Porcelains: Effect of Alumina Additions on Thermal Diffusivity and Elastic Constants

S. Bribiesca,[a]* R. Equihua[a] and L. Villaseñor[b]

[a]Departamento de Cerámica, Instituto de Investigaciones Metalúrgicas, Universidad Michoacana, Apdo. Postal 52-B, Morelia Michoacán, 58000, México
[b]Instituto de Física y Matemáticas, Universidad Michoacana, Apdo. Postal 2-82, Morelia Michoacán, 58040, México

(Received 1 September 1998; accepted 12 December 1998)

Abstract

The open-photoacoustic-cell technique to measure thermal diffusivity is described in detail. We have applied it to the measurement of thermal diffusivity of porcelain samples with four different alumina additions in the range 0–15 wt% and fired at four temperatures in the range 1270–1350°C. Thermal diffusivity is shown to vary from $4{\cdot}1\times10^{-7}$ $m^2 s^{-1}$ *for a classical triaxial porcelain to* $6{\cdot}4\times10^{-7}$ $m^2 s^{-1}$ *for 15 wt% alumina addition made mainly at the expense of quartz when the firing temperature was 1325°C. The values of thermal diffusivity are found to be well correlated with the values of the shear and Young's modulus. Good correlation was also observed among the measured values for thermal diffusivity and those for density and mullite to quartz ratio. We conclude that the open-photoacoustic-cell technique has enough sensitivity to detect small changes in composition and microstructure of materials as complex as porcelains.* © *1999 Elsevier Science Limited. All rights reserved*

Keywords: photoacoustic effect, thermal conductivity, porcelain, insulators, elastic constants.

1 Introduction

Porcelains are widely used in household, laboratory and industrial applications, in particular, electrical porcelains are still extensively used as insulators in electrical transmission lines mainly due to the high stability of their electrical, mechanical and thermal properties in presence of harsh environments. Research on the dependence of several physical properties of porcelains with different chemical compositions and preparation procedures is important,[1–4] partly due to the rising need of optimizing the material for a given application at the lowest cost. Among the various physical properties, thermal diffusivity is one of the most sensitive to compositional, microstructural and processing variables,[5] however, studies on the behavior of thermal diffusivity as a function of composition and preparation procedure are scarce in the literature. Thermal diffusivity, α, is the parameter that measures the rate of heat diffusion in a sample, it represents a genuine and important bulk property of the material which is directly related to thermal conductivity, another important transport property, by means of the equation[6]

$$\alpha = \frac{k}{\rho c}, \tag{1}$$

where k is thermal conductivity, ρ is density and c is specific heat at constant pressure of the sample. The measurement of thermal diffusivity is usually preferred over the measurement of thermal conductivity because the latter involves heat fluxes that are difficult to control; on the other hand, thermal conductivity can be obtained from eqn (1) as density and specific heat can be measured or calculated relatively simply and accurately.[7,8] Among the numerous techniques for measuring thermal diffusivity, those based on temperature probes to monitor temperature variations in the sample are plagued with systematic errors because the probes

*To whom correspondence should be addressed.

may distort heat fluxes in ways that are difficult to model. The photoacoustic (PA) effect provides the basis for a technique that is free of this inconvenience with the additional advantage of requiring relatively inexpensive laboratory equipment.

The PA effect occurs when periodically interrupted radiation is absorbed by a solid sample giving rise to variations in the temperature of the sample. The variation in the pressure of the air in contact with the surface of a sample confined in a closed volume, referred to as PA cell, produces a PA signal in the form of acoustic waves. In the optical case the PA signal is due to the periodic deposition of heat by light, the so called photothermal (PT) effect which is caused by non-radiative de-excitation processes following the absorption of light by the sample. Monitoring the amplitude and phase of the acoustic waves by means of a sensitive microphone coupled to the cell provides information about various physical properties of the sample, including its thermal diffusivity. This is due to the fact that the PA signal depends not only on the sample's optical absorption coefficient and its light-into-heat conversion efficiency but also on the way the heat diffuses through the sample. A comprehensive review on PA phenomena and their applications can be found in the following books and review papers.[9–13] Although the PA effect was discovered over a hundred years ago,[14] a proper understanding and modeling of the effect was not given until the decade of the 1970s,[15] and only recently it has been shown to provide the basis for a simple and reliable technique for non-destructive measurement of thermal diffusivity of materials as diverse as glasses,[16] semiconductors,[17] polymers[18] and ceramics[19] among other materials.

In the present paper we investigate and describe the use of a modification of the traditional PA technique to measure thermal diffusivity; this new technique is called the open-photoacoustic-cell (OPC) method.[20] We used it to study thermal diffusivity at room temperature of triaxial porcelains with four different additions of alumina in the range 0–15 wt% and fired at four temperatures in the range 1270–1350°C. The OPC approach consists in the use of a commercial electret microphone[21] as the PA cell itself. The open-cell approach simplifies the process of installation and removal of the sample, and, unlike the traditional PA techniques, it does not require any machining. The application of the OPC technique to these porcelains manufactured with slightly different chemical compositions and sintering temperatures constitutes a valuable exercise to detect possible systematic errors associated with the experimental technique as applied to complex solids. We found the OPC technique to be sufficiently sensitive to detect changes in the values of thermal diffusivity at room temperature of the porcelain samples studied; these measurements show a strong correlation with density, elastic constants and ratio of mullite to quartz which were measured independently. The OPC technique can also be used as the basis of a simple, precise, and inexpensive tool for quality control in the manufacturing of porcelains in particular, or any other solid material in general.

2 Experimental Procedure

2.1 Preparation of specimens

Four bodies with different compositions of alumina (reactive agent 99·86% pure), kaolin (from Jalisco, México), ball clay (from Kentucky, USA), feldspar and quartz (both from Guanajuato, México) were prepared with the weight percentages shown in Table 1. These raw materials had a wide distribution of particle sizes in the range of 1–12 μm to ensure good compactness of the final bodies. The chemical composition of these raw materials is shown in Table 2.

As shown in Table 1, the composition of the first body corresponds to the conventional composition of electrical porcelains; the alumina addition on the other bodies was made at expense of quartz, and slightly of feldspar for the fourth body. The raw

Table 1. Weight percentage formulation of the four samples studied in this article

	Kaolin (wt%)	*Ball-clay (wt%)*	*Feldspar (wt%)*	*Quartz (wt%)*	*Alumina (wt%)*
Body 1	30	20	25	25	0
Body 2	30	20	25	20	5
Body 3	30	20	25	15	10
Body 4	30	20	20	15	15

Table 2. Chemical composition of the raw materials used for the preparation of the samples

Chemical composition (mole%)	*Kaolin*	*Ball-clay*	*Feldspar*	*Quartz*	*Alumina*
SiO_2	68·580	72·035	76·706	97·310	0·051
Al_2O_3	27·000	23·628	11·690	1·330	99·862
K_2O	0·980	0·399	7·409	0·376	—
Na_2O	0·176	—	3·599	0·561	—
Fe_2O_3	0·080	0·532	0·099	0·006	0·087
Rb_2O	—	—	0·022	0·020	—
BaO	0·030	—	0·017	0·003	—
CaO	0·510	0·544	0·398	0·390	—
TiO_2	0·591	1·846	0·058	0·004	—
P_2O_5	0·987	0·079	—	—	—
SrO	0·114	—	—	—	—
Cr_2O_3	0·010	—	—	—	—
MgO	0·940	0·937	—	—	—
Total	99·998	100·000	99·998	100·000	100·000

materials were wet mixed for 24 h by means of a mechanical agitator to obtain good homogenization and the resulting suspension was dried at 100°C for 2 h and pressed into discs of 30 mm diameter by using a pressure of $31{\cdot}2\times10^6$ Pa. The discs were subsequently sintered at four different temperatures (1270, 1300, 1325 and 1350°C) and soaked for 2 h. The densities of the samples were obtained by dividing their measured masses by their volumes as calculated from their geometrical dimensions.

2.2 Measurement of elastic constants

The elastic constants of the porcelain discs were measured by the non-destructive impulse excitation technique (Grindo-Sonic System, J.W. Lemmens Inc., St Louis, MO). The method is based on the excitation of the homogeneous test sample by means of a light mechanical impulse; the resulting vibration, which depends on the nature, geometry and mass of the material, is picked up and analyzed by the instrument to select and measure the fundamental mode of oscillation. This instrument, which meets standards (American Society for Testing and Materials designation C 1259, West Conshohocken, PA), provides the values of the shear and Young's modulus once the geometrical dimensions of the sample are specified.

2.3 Phase characterization

The mullite to quartz ratio of the crystalline phases of the porcelain discs was measured by X-ray powder diffractometry. The samples were ground and the fine powder was analyzed with a Philips diffractometer (Philips Electronic Instruments, Mahwah, NJ) with Cu(K_α) radiation at 35 KV and 15 mA. A scanning electron microscope (JEOL, Model 6400, Palo Alto, CA) was used to analyze the microstructure of the porcelain samples. As a preparation for scanning electron microscopy (SEM) analysis, the samples were polished and HF etched to dissolve the glassy matrix and to enhance their crystalline morphologies; afterwards they were glued onto the cylindrical holder and covered with a thin film of gold.

2.4 Measurement of thermal diffusivity

The experimental array used for the PA measurement of thermal diffusivity at room temperature is shown schematically in Fig. 1. The porcelain samples were reduced to discs of about 1 cm^2 of cross section and about 300 μm of thickness by using TiC abrasive paper. The sample to be measured was placed atop a commercial electret microphone element (cat. no. 270-092B, Radio Shack), shown schematically in Fig. 2. This microphone serves as the air-tight OPC. The sample was illuminated

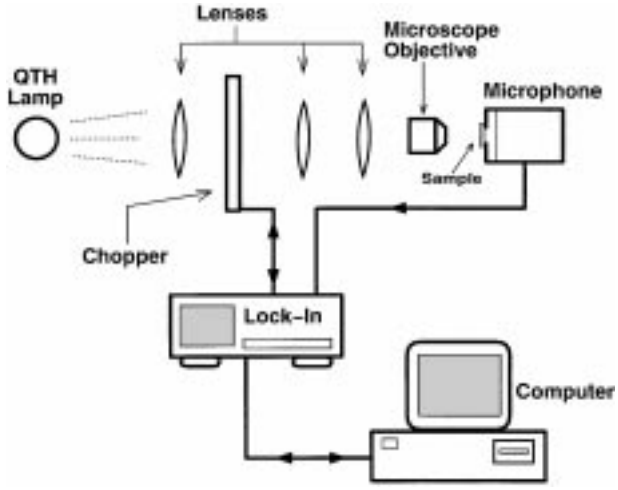

Fig. 1. Schematic view of the experimental setup used for thermal diffusivity measurements.

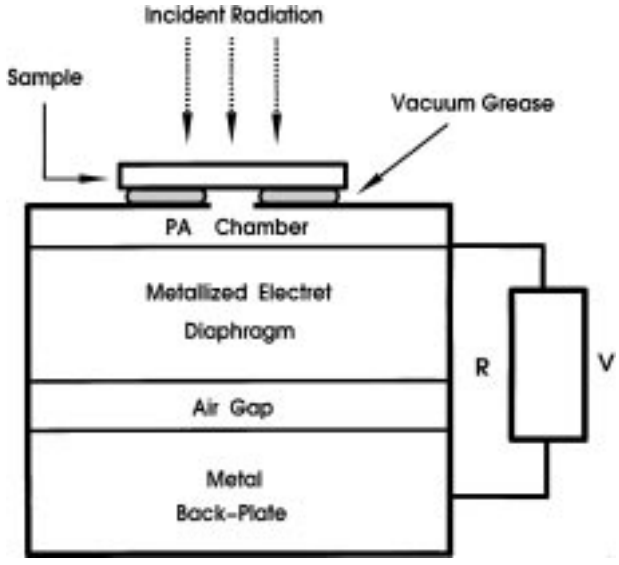

Fig. 2. Schematic view of the electret microphone used as the open photoacoustic cell in the measurements of thermal diffusivity.

with a chopped (chopper controller model SR540, Stanford Research Systems) light beam from a 250 W quartz–tungsten–halogen (QTH) lamp. A thin circular aluminum foil (14 μm thick and 7 mm diameter) was previously attached (using a thin layer of thermal paste) to the front surface of the sample to insure that the heat produced by the photothermal effect was deposited only at the surface of the sample. The amplitude and phase of the PA signal were measured by a *lock-in* amplifier (model SR850, Stanford Research Systems) connected to a personal computer (PC) by means of a GPIB (General Purpose Interface Bus) port (model AT-GPIB, National Instruments). The data acquisition process was controlled by means of a data acquisition program running on the PC; this program was written in the graphical language called LabView (National Instruments).

In the case of the OPC array such as the one we use, schematically shown in Figs 1 and 2, a straightforward application of the one-dimensional thermal diffusion model of Rosencwaig and Gersho[15] to an optically opaque sample, of thickness l and thermal diffusivity α, for the case that the sample is thermally thick [meaning that the diffusion frequency $\alpha/(\pi l^2)$ is much lower than the chopper frequency f] predicts that the phase difference between the PA signal from the microphone and the reference signal from the chopper varies with the chopper frequency, f, as

$$\theta = \theta_o - af^{1/2}; \tag{2}$$

the same model predicts that the PA amplitude, S_{model}, varies as

$$S_{\text{model}} = \frac{A}{f} e^{-a\sqrt{f}}, \tag{3}$$

with

$$a = \sqrt{\pi l^2/\alpha} \tag{4}$$

Therefore, the value for a can be obtained by fitting the phase data to eqn (2) or, alternatively, the amplitude data to eqn (3); subsequently, the thermal diffusivity value can be extracted from eqn (4) as the sample thickness is independently measured with a dial indicator (model 2110F, Mitutoyo).

In the case that thermal diffusivity is extracted from the amplitude data by means of eqn (3), care must be exercised to account for the uneven frequency response of the microphone to acoustic vibrations; this uneven response is present in practically all microphones, especially at low frequencies in the 8–200 Hz range. Therefore, the PA amplitude measurements must be corrected by means of a multiplicative function, $\chi^{-1}(f)$, to account for this effect. In order to obtain the specific response function of the microphone we used, $\chi(f)$, we applied the PA effect to an optically opaque sample in the thermally thin case where the one-dimensional Rosencwaig and Gersho PA model[15] predicts that the PA amplitude at the microphone output, S_{model}, varies as

$$S_{\text{model}} = \frac{A}{f^{3/2}}, \tag{5}$$

where f is the modulation frequency and A is a constant. In this context, thermally thin means that the time required for the heat to diffuse from one side of the sample to the other, $\pi l^2/\alpha$, is much smaller than the modulation period of the chopper, $1/f$. This requirement is well satisfied by a copper foil of 100 μm of thickness which has a diffusion time of only 273 μs, i.e. short compared with the modulation period of 125–5 ms for a frequency range of 8–200 Hz. Therefore, the microphone response function was obtained as the ratio of the measured PA amplitude, S_{exp}, to the model-predicted amplitude, S_{model}, which for the case of an opaque and thermally thin sample is given by the following equation:

$$S_{\text{exp}} = \chi(f) S_{\text{model}} = \chi(f) \frac{A}{f^{3/2}} \tag{6}$$

Figure 3 shows the response function obtained this way; all experimental PA amplitudes used to measure α, as discussed in the next paragraph, are always divided by the microphone response function so that proper comparisons with the theoretical model can be made.

Figure 4 shows the data obtained for the PA amplitude, actually $\ln(fS)$, and the phase angle as a function of $\sqrt{f}$ for the sample with 10 wt% alumina addition fired at 1300°C; this sample was reduced to a thickness of 275 ± 5 μm and a cross section of about 1 cm^2. The solid straight lines are

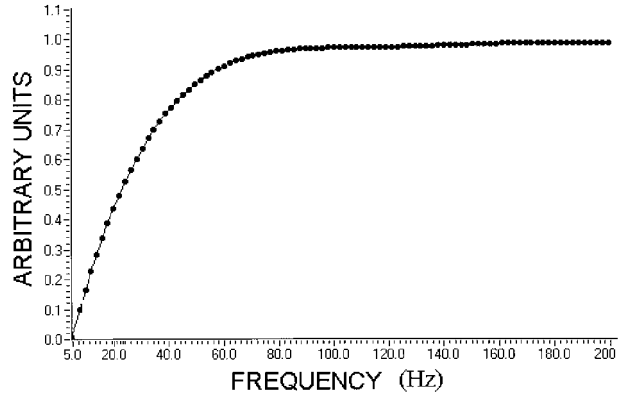

Fig. 3. Microphone response function in the frequency range of the photoacoustic measurements of thermal diffusivity.

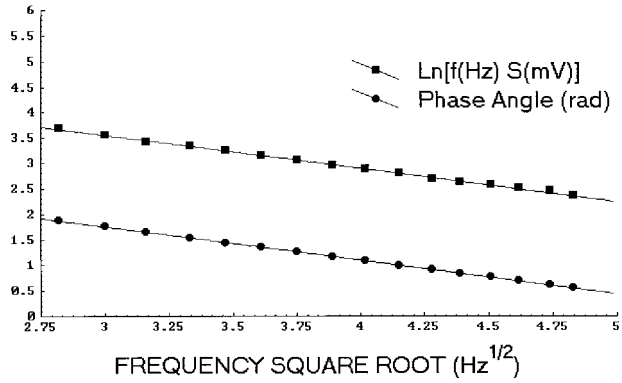

Fig. 4. Typical data for $\ln(fS)$ and the phase angle as a function of $\sqrt{f}$ for the sample with 10 wt% alumina addition fired at 1300°C. The solid straight lines are fits of the data to eqn (2), for the phase angle and eqn (3), for the PA amplitude. The value of thermal diffusivity derived from the slopes of the fit lines by means of eqns (2)–(4) was $\alpha = 5{\cdot}5 \pm 0{\cdot}3 \times 10^{-7}$ m^2 s^{-1}.

fits of the data to eqn (3), for the PA amplitude, and to eqn (2), for the phase angle between the PA signal and the reference signal from the chopper. The fits were obtained by the least squares method. The slopes of the two fitted lines were $-0{\cdot}656$; by using eqn (4) we derived a value for the thermal diffusivity of $\alpha = 5{\cdot}5 \pm 0{\cdot}3 \times 10^{-7}\,m^2\,s^{-1}$. The 5% error shown was the quadratic sum of the fit error and the error on the thickness, each being of the order of 3·5%. As a consistency crosscheck, we note that the threshold frequency that separates the thermally thin and thermally thick cases for an optically opaque sample, given by $f_c = \alpha/(\pi l^2)$ is about 2·3 Hz, so that the application of the model corresponding to a thermally thick sample is justified in the frequency range of 8–23 Hz in which the measurement was performed; in this range thermoelastic effects can be neglected, however, at higher frequencies the model we use stops being valid as thermoelastic effects become dominant.[18] The values of thermal diffusivity for the other samples were obtained in a similar way. The OPC technique described above has been extensively checked by the authors on reference materials of known thermal diffusivity, such as aluminum, copper and stainless steel; in all these cases the measured values were in good agreement with the values reported in the literature.

3 Results and Discussion

Table 3 lists the data for density, thermal diffusivity at room temperature, Young's modulus, shear modulus and ratio of mullite to quartz for the bodies with 0, 5, 10 and 15 wt% alumina additions fired at 1270, 1300, 1325 and 1350°C, respectively. The minimum value of thermal diffusivity was $4{\cdot}1\times10^{-7}\,m^2\,s^{-1}$ for the body with 0 wt% alumina addition fired at 1325°C, while the maximum value was $6{\cdot}4\times10^{-7}\,m^2\,s^{-1}$ for the body with 15 wt% alumina addition also fired at 1325°C. This 56% increase, along with the general increase of thermal diffusivity with the amount of alumina addition for a constant firing temperature, support the fact that thermal diffusivity is indeed a sensitive parameter to changes in composition of porcelains. Thermal diffusivity is also sensitive to changes in sintering temperature as evidenced by the body with 15 wt% alumina addition which shows an increase from $4{\cdot}7\times10^{-7}\,m^2\,s^{-1}$ for a firing temperature of 1270°C to $6{\cdot}4\times10^{-7}\,m^2\,s^{-1}$ for a firing temperature of 1325°C, i.e. a 36% change, while the bodies with alumina additions in the range 0–10 wt% also showed an increase in thermal diffusivity when the firing temperature was increased from 1270 to 1300°C.

For the full 0–15 wt% range of alumina additions studied we obtained values of thermal diffusivity strongly correlated with the values of shear and Young's modulus as can be seen from Table 3. The sample with 0 wt% alumina addition fired at 1325°C showed the minimum values of the Young's modulus (43·6 GPa), shear modulus (18·7 GPa), and thermal diffusivity ($4{\cdot}1\times10^{-7}\,m^2\,s^{-1}$). Likewise, the sample with 15 wt% alumina addition fired at 1325°C showed the maximum value of thermal diffusivity, and had values of the shear and Young's modulus very close (98%) to the maximum values obtained among the samples studied. This strong correlation indicates that the OPC technique we used to measure thermal diffusivity indeed provides measurement values in a consistent way.

As thermal and mechanical properties are sensitive to the value of sintering temperature, it is important to use the optimum firing temperature to make effective use of the amount of alumina addition. Our results indicate that the optimum firing temperature for the bodies with 0–10 wt% alumina additions is around 1300°C while the optimum temperature for the body with 15 wt% alumina addition is around 1325°C. Exceeding the optimum firing temperatures produced a decrease in the samples' densities as can be seen from Table 3. In fact, bloating was observed on the samples with 0–10 wt% alumina additions fired at 1325°C as well as on the bodies with 10 and 15 wt% alumina additions fired at 1350°C.

The presence of the glassy phase along with the mullite, quartz and corundum crystals embedded on it were clearly identified by our X-ray powder diffractometry analyses. The ratio of mullite to quartz shown in Table 3 is the ratio of the highest peak amplitudes of the two materials in the X-ray diffractogram. Mullite crystals were also seen as fine needle-like shapes in all directions in our SEM studies. The needle-like shape of mullite crystals is well understood in terms of its atomic structure. Excepting the body with 15 wt% alumina addition fired at 1270°C (presumably because this temperature was not high enough for sintering, i.e. the sample was underfired), the density and the ratio of mullite to quartz of all the bodies increased with alumina additions for a given firing temperature; this means that more mullite was formed when there was more alumina available as long as the firing temperature was high enough to enrich the glassy phase with SiO_2, which in turn contributes to the synthesis of mullite. An increase in alumina contents (with a small average particle size of 1 μm) led to a better compactness of the material due to the increase of fine grained mullite in the glassy matrix. Our results agree with the well known

Table 3. Measured data for density, thermal diffusivity, Young's modulus, shear modulus and ratio of mullite to quartz for the porcelain samples studied

Body	*Density* ϱ *(×10³ Kg m⁻³)*	*Thermal diffusivity* α *(×10⁻⁷ m² s⁻¹)*	*Young's modulus* E *(GPa)*	*Shear modulus* G *(GPa)*	*M/Q*
1270°C					
P1-(0%)	2·13	4·4 ± 0·2	47·9	20·4	0·170
P2-(5%)	2·16	4·8 ± 0·2	51·6	21·8	0·311
P3-(10%)	2·20	5·3 ± 0·3	53·0	22·4	0·355
P4-(15%)	2·10	4·7 ± 0·3	46·4	19·8	0·253
1300°C					
P1-(0%)	2·11	4·4 ± 0·2	49·6	21·0	0·156
P2-(5%)	2·18	5·0 ± 0·2	56·8	24·0	0·226
P3-(10%)	2·22	5·5 ± 0·3	61·0	25·6	0·333
P4-(15%)	2·31	5·8 ± 0·3	62·1	26·1	0·357
1325°C					
P1-(0%)	1·92	4·1 ± 0·2	43·6	18·7	0·283
P2-(5%)	2·00	4·4 ± 0·2	50·3	21·2	0·300
P3-(10%)	2·14	5·3 ± 0·3	57·8	24·0	0·422
P4-(15%)	2·27	6·4 ± 0·3	64·9	27·2	0·500
1350°C					
P3-(10%)	2·02	4·9 ± 0·2	53·4	22·3	0·433
P4-(15%)	2·23	6·1 ± 0·3	66·3	27·6	0·571

fact[22] that the mechanical strength of a porcelain can be raised by increasing the amount of mullite crystals at the expense of the glassy phase. This rise in the shear and Young's modulus can be linked to the reinforcing effect of the needle-like mullite crystals on the structure of the porcelain; this effect is similar to the reinforcing effect of long glass fibers in fiberglass. From our study, we conclude that besides the elastic constants, thermal diffusivity also improves with alumina additions but only up to the point where the optimum firing temperature is used. Overfiring the material gave rise to a decrease in density (increase in porosity) even though the ratio of mullite to quartz kept increasing. The increase of porosity in the overfired samples was accompanied by a decline in thermal diffusivity and elastic constants, except in the case of the sample with 15 wt% alumina addition overfired at 1350°C; in the latter case thermal diffusivity showed a decline as a consequence of the lower density but the elastic constants showed a small increase. This result can be understood by noting that the ratio of mullite to quartz increased from 0·500 to 0·571 as can be seen from Table 3 and presumably the effect of the lower density in the elastic constants is somewhat compensated by the greater amount of mullite crystals, whereas the behavior of thermal diffusivity is mainly dominated by porosity. In addition, we observed that the mullite needle-like crystals were slightly longer in the overfired samples than in the samples fired at optimum temperature.

The correlation among the various physical properties discussed above can be qualitatively understood on physical grounds, quantitative models are better tested with simpler solids where parameters, such as porosity, are controlled more systematically. At room temperature, where the photon conduction across pores can be neglected, the qualitative effect of a greater porosity on thermal diffusivity and elastic constants can be attributed to the decrease in the phonon mean free path and simultaneously to the decrease in rigidity of the solid.

4 Conclusions

We have described in detail the use of a novel open-photoacoustic-cell technique to measure thermal diffusivity at room temperature of 12 samples of triaxial porcelains prepared with alumina additions in the range 0–15 wt% fired at four different temperatures in the range of 1270–1350°C. We have demonstrated that these small additions of alumina produce noticeable changes in the values of thermal diffusivity which were strongly correlated with the values of the shear and Young's modulus. The OPC technique makes use of an electret microphone as the photoacoustic cell in place of the more traditional closed photoacoustic chamber. We have checked that this technique indeed produces thermal diffusivity values in agreement with the values reported from other measuring methods when it is applied to standard materials, such as aluminum, copper and different kinds of steels. Our study validates the fact that this computer-automated technique is sensitive enough to detect changes in thermal diffusivity due to small

changes in composition and sintering temperature of solids as complex as porcelains. The strong correlation found between thermal diffusivity and elastic constants indicates that the OPC technique we used to measure thermal diffusivity provides measurement values in a consistent way.

We conclude that the OPC technique constitutes a viable candidate to perform thermal characterization of porcelains in general; it has the additional advantage of providing relatively precise measurements in a short time interval using relatively inexpensive laboratory equipment. The main advantages of the OPC technique with respect to other more traditional techniques are the following: (a) it is non-destructive; (b) it requires small samples (foils of about 1 cm^2 of cross section and 300 μm of thickness); (c) it is well suited to the measurement of thermal diffusivity for heat flow along each of the three main axes of non-isotropic materials; (d) it provides relatively precise results (around 3·5% error); (e) the laboratory equipment required is relatively inexpensive; and (f) the measurements can be performed in a completely automated way in a short time interval (about 5 min per sample). The OPC technique can also be used as the basis of a simple, precise, and inexpensive tool for quality control in the manufacturing of porcelains.

As the values of thermal diffusivity and elastic constants are sensitive to the sintering temperature used, it is important to use the optimum firing temperature to make effective use of the amount of alumina addition in each specific case. Our results indicate that the optimum firing temperature for the bodies with 0–10 wt% alumina additions is around 1300°C while the optimum firing temperature for the body with 15 wt% alumina addition is around 1325°C. Exceeding the optimum firing temperatures produced a decrease in the samples' densities accompanied by a general decrease of thermal diffusivity and elastic constants. Our results clearly favor the view that mullite plays an important role in improving thermal diffusivity and the elastic constants of electrical porcelains with even small amounts of alumina additions.

Acknowledgements

We would like to thank Mr R. Hernández and Mr C. Pacheco for helpful technical assistance during the elaboration of this work. This work was supported by the Universidad Michoacana through the Coordination of Scientific Research and the Universidad Autónoma del Estado de Morelos.

References

1. Kato, E., Satoh, T., Ohira, O. and Kobayashi, Y., Compositions for strengthening porcelain bodies in alumina–feldspar–kaolin system. *Brit. Ceram. Trans. J.,* 1994, **93**, 49–52.
2. Hamano, K., Hatano, A. and Okada, S., High mechanical strength porcelain body prepared from Amakusa pottery stone containing soda feldspar. *J. Ceram. Soc. Jpn*, 1993, **101**, 1012–1017.
3. Kobayasi, Y., Ohira, O., Satoh, T. and Kato, E., Effect of quartz on the sintering and bending strength of the porcelain bodies in quartz–feldspar–kaolin system. *J. Ceram. Soc. Jpn,* 1994, **102**, 384–389.
4. Maiti, K. N. and Kumar, S., Microstructure and properties of a new porcelain composition containing crystallising glasses as replacement for feldspar. *Brit. Ceram. Trans. J.,* 1992, **90**, 19–24.
5. Touloukian, Y. S., Powell, R. W., Ho, C. Y. and Nicolaou, M., Thermophysical properties of matter. *The TPRC Data Series, Vol. 10, Thermal Diffusivity*. Plenum Press, New York, 1973.
6. Bejan, A., *Heat Transfer*. John Wiley & Sons, New York, 1993, pp. 9–10.
7. Maglic, K. D., Cezairliyan, A. and Peletsky, V. E., *Compendium of Thermophysical Property Measurement Methods 1: Survey of Measurement Techniques*. Plenum Press, New York, 1984, pp. 457–460.
8. Hatta, I., Heat capacity measurements by means of thermal relaxation methods in medium temperature range. *Rev. Sci. Instrum.*, 1979, **50**, 292–295.
9. Rosencwaig, A., *Photoacoustics and Photoacoustic Spectroscopy*. John Wiley & Sons, New York, 1980.
10. Mandelis, A., *Photoacoustic and Thermal Wave Phenomena in Semiconductors*. North-Holland, New York, London, 1987.
11. Bicanic, D., *Photoacoustic and Thermal Wave Phenomena III*. Springer–Verlag, Berlin, Heidelberg, New York, 1992.
12. Vargas, H. and Miranda, L. C. M., Photoacoustic and related photothermal techniques. *Phys. Rep.*, 1988, **161**, 43–101.
13. Fork, D. C. and Herbert, S. K., The application of photoacustic techniques to studies of photosynthesis. *Photochem. Photobiol.*, 1993, **57**, 207–220.
14. Bell, A. G., Upon the production of sound by radiant energy. *Phil. Mag.*, 1881, **11**, 510–528.
15. Rosencwaig, A. and Gersho, A., Theory of the photoacustic effect with solids. *J. Appl. Phys.*, 1976, **47**, 64–69.
16. Bento A. C., Vargas, H., Aguilar, M. M. F. and Miranda, L. C. M., Photoacoustic characterization of quartz. *Phys. Chem. Glasses*, 1987, **28**, 127–129.
17. Pinto-Neto, A., Vargas, H., Leite, N. F. and Miranda, L. C. M., Photoacoustic characterization of semiconductors: transport properties and thermal diffusivity in GaAs and Si. *Phys. Rev. B*, 1990, **41**, 9971–9980.
18. Leite, N. F., Cella, N., Vargas, H. and Miranda, L. C. M., Photoacoustic measurements of thermal diffusivity of polymer foils. *J. Appl. Phys.*, 1987, **61**, 3025–3027.
19. Contreras, M. E., Serrato, J., Zarate, J., Pacheco, C. and Villaseñor, L., Photoacoustic thermal characterization of lime-partially stabilized zirconia. *J. Am. Ceram. Soc.*, 1997, **80**, 245–249.
20. da Silva, M. D., Bandeira, I. N. and Miranda, L. C. M., Open-cell photoacoustic radiation detector. *J. Phys. E: Sci. Instrum.*, 1987, **20**, 1476–1478.
21. Sessler, G. M., Electrostatic microphones with electrot foil. *J. Acoust. Soc. Am.*, 1963, **35**, 1354–1357.
22. Kreimer, D. B. and Chistyakova, T. I., Influence of phase composition of aluminous porcelain on its mechanical strength. *Glass and Ceramics*, 1990, **46**, 489–491.